

Ion fluxes and energies in inductively coupled radio-frequency discharges containing CHF_3

Yicheng Wang,^{a)} M. Misakian, A. N. Goyette, and J. K. Olthoff^{b)}

Electronics and Electrical Engineering Laboratory, National Institute of Standards and Technology, Gaithersburg, Maryland 20899-8113

(Received 16 June 2000; accepted for publication 30 August 2000)

Measurements of ion energy distributions, relative ion intensities, and absolute total ion current densities were made at the grounded electrode of an inductively coupled Gaseous Electronics Conference (GEC) radio-frequency reference cell for discharges generated in CHF_3 and its mixtures with argon. In general, the dominant ion species detected were not due to direct ionization of the CHF_3 feed gas. Results are presented for plasmas generated with and without a confining quartz annulus that has recently been used to extend the operating parameter range of inductively coupled GEC cells for certain etching gases. Compared to similar plasmas generated without the annulus, the presence of the ring increases the ion flux density by approximately a factor of 2, and increases the mean ion energies. The presence of the ring does not significantly affect the measured relative ion intensities. [S0021-8979(00)04123-2]

I. INTRODUCTION

Different fluorocarbon gases are commonly used in the fabrication of semiconductor devices for the etching of silicon and silicon dioxide and for the deposition of fluorocarbon films. Trifluoromethane (CHF_3) is one such gas (see, for example, Refs. 1 and 2) that is sometimes used because of its shorter atmospheric lifetime compared to other etching gases.³ Ion bombardment plays a key role in these processes, and the identity, energy, and flux of the bombarding ions are relevant to an understanding of the etching and/or deposition processes. Two recent studies^{4,5} have investigated the composition of the ion fluxes sampled from the side of inductively coupled plasma (ICP) sources using CHF_3 as a feed gas. Li *et al.*⁵ presented measurements of mass-selected ion fluxes obtained in a high power ICP reactor, while Jayaraman *et al.*⁴ reported relative ion fluxes generated in a lower power reactor. In this article, we present relative ion flux densities, mass-analyzed ion energy distributions (IEDs), and absolute ion flux densities measured in inductively coupled plasmas generated in pure CHF_3 and in mixtures of CHF_3 and argon. These data are useful in understanding the chemistry of such discharges, and may be used to validate plasma models.

The plasmas investigated here were produced in a Gaseous Electronics Conference (GEC) radio-frequency (rf) reference cell⁶ that was modified to house an inductively coupled plasma source.⁷ Data from these reactors have been successfully used to advance the modeling of ICP reactors (see, for example, Refs. 8–11). However, researchers using such GEC-ICP cells have found that the range of plasma parameters (pressure, power, gas composition) for which a stable plasma could be sustained in many common etching gases (e.g., CF_4 , C_2F_6 , $c\text{-C}_4\text{F}_8$, and CHF_3) was extremely

limited. Recently, a quartz annulus mounted around the upper quartz window has been utilized in some GEC-ICP cells in order to extend the range of stable plasma conditions for these gases.^{4,12,13} Here we report extensive ion data under both experimental arrangements (with and without the added quartz ring). Comparison of the results show that the presence of the ring affects the total ion flux and the mean ion energies, but generally not the relative composition of the ion flux.

II. EXPERIMENT

The discharges studied here were generated in a GEC rf reference cell reactor whose upper electrode has been replaced with a five-turn planar rf-induction coil behind a quartz window to produce inductively coupled discharges.⁷ The design of the GEC rf reference cell is described in detail elsewhere.^{6,14} A quartz annulus was developed for use in the GEC-ICP cell to allow the generation of plasmas in electro-negative gases over a broader range of pressures and powers. The reactor with the ring mounted to the upper quartz window of the source is depicted schematically in Fig. 1. Also shown is the ion energy analyzer and mass spectrometer attached to the lower electrode. The feed gas enters the cell through one of the 2.75 in. side flanges and is pumped out through the 6 in. port attached to a turbomolecular pump. The gas pressure is maintained by a variable gate valve between the GEC cell and the pump. Mass flow controllers regulated the flow, which was maintained at $3.73 \mu\text{mol/s}$ (5 sccm) for pure CHF_3 discharges or $7.45 \mu\text{mol/s}$ (10 sccm) for mixtures of CHF_3 with Ar.

A 13.56 MHz voltage is applied to the coil through a matching network. The rf power values presented in this article are the net power to the matching network driving the coil. The actual rf power dissipated in the plasma has been determined to be approximately 80% of the power listed.⁷

^{a)}Electronic mail: yicheng.wang@nist.gov

^{b)}Electronic mail: james.olthoff@nist.gov

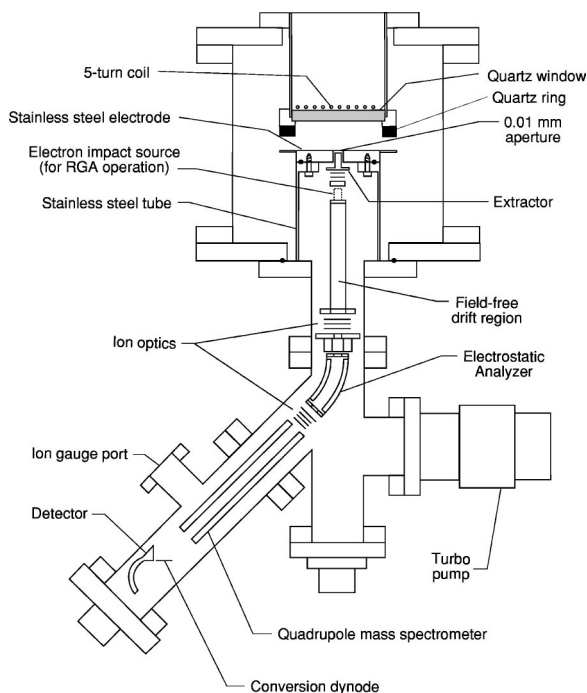


FIG. 1. Schematic diagram of the inductively coupled GEC rf reference cell with the ion-energy analyzer and mass spectrometer appended to the modified lower electrode. The quartz annulus (ring) around the upper quartz window is shown in black.

The lower electrode, through which the ions are sampled, is grounded to the vacuum chamber.

The ion sampling arrangement is identical to that used to study inductively coupled plasmas in other fluorocarbon gases,^{12,13,15} and in Ar, N₂, O₂, Cl₂, and their mixtures.¹⁶ Ions are sampled through a 10 μ m diam orifice in a 2.5 μ m thick nickel foil spot welded into a small counterbore located at the center of the stainless steel lower electrode. For IED measurements, the ions that pass through the orifice are mass selected by the quadrupole mass spectrometer after being energy analyzed by the 45° electrostatic energy selector. The IEDs measured in this manner are essentially ion-flux energy distributions.¹⁷

Past experience with the ion energy analyzer indicates that the ion transmission is nearly constant over the energy ranges observed here.¹⁷ A mass-dependent transmission correction factor, however, was applied to the highest mass ions (mass >40 u) in order to compensate for some decrease in the ion transmission of the quadrupole mass spectrometer with increasing mass. This factor was approximately 2 for CF₃⁺ (mass 69).

For total ion current measurements (i.e., all ion current passing through the sampling orifice), the ion optic elements at the front of the ion energy analyzer are biased such that the current passing through the sampling orifice is collected on the extractor element (the first ion optic element behind the electrode surface), and is measured using an electrometer. Total ion current measurements exhibit a reproducibility of $\pm 15\%$.

The total ion current is partitioned into mass channels according to the mass spectrum of ions. The absolute intensities of the measured IEDs are then determined by scaling

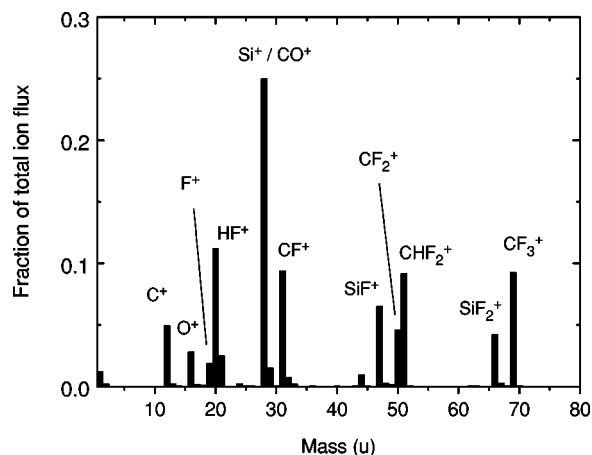


FIG. 2. Mass spectrum of ions sampled from a CHF₃ plasma through a hole in the grounded electrode of a GEC-ICP cell. The plasma parameters were 200 W and 0.67 Pa (5 mTorr), and the quartz annulus around the upper quartz window (see Fig. 1) was in place. The mass spectra obtained under the same plasma conditions without the quartz annulus were nearly identical.

the measured values of the ion current for the appropriate mass channel to the total ion current. The ion flux densities presented here are derived by dividing the total measured ion current by the area of the 10 μ m diam sampling hole.

III. RESULTS AND DISCUSSION

A. CHF₃ plasmas

Figure 2 shows the mass spectrum of ions sampled from a 200 W, 0.67 Pa (5 mTorr), CHF₃ plasma with the quartz annulus in place. The mass spectrum obtained without the ring (not shown) is almost identical, indicating that relative intensities of the different ions are nearly unchanged for each arrangement.

The dominant ion in the mass spectrum is at mass 28 u, which corresponds to either Si⁺ or CO⁺. (N₂⁺ is not a likely contributor to the mass 28 signal since no N⁺ is observed in the mass spectrum.) Since Si possesses significant isotopes at masses 29 and 30, an analysis of the ratios of the peaks near 28 u indicates that the mass 28 peak is due to a nearly equal mixture of Si⁺ and CO⁺. A similar analysis of the mass 47 and mass 66 peaks indicates that they consist primarily of SiF⁺ and SiF₂⁺, respectively. None of these ions is due to direct ionization of the feed gas, but are the result of the etching of the quartz window in the GEC-ICP source. This agrees with previous observations of significant quartz window etching in inductively coupled plasma sources using CHF₃ feed gases.⁵ While Si⁺/CO⁺ has been observed as a significant ion signal in all fluorocarbon plasmas generated in our GEC-ICP cell,^{12,15} the magnitude of the mass 28 peak is significantly larger in hydrogen-containing plasmas, such as CHF₃ and CF₃CH₂F, than in plasmas generated in perfluorinated gases (i.e., CF₄, C₂F₆, and *c*-C₄F₈). The reason for this is difficult to assess since the surface interactions in CHF₃ plasmas reflect a complex combination of deposition and etching that depends strongly on the plasma conditions.¹⁸ However, there is some evidence that CHF₃

plasmas can etch SiO_2 more effectively than CF_4 plasmas under certain low-bias (low ion energy) conditions.¹⁹

Similarly, HF^+ is another “secondary” ion exhibiting significant intensity in the CHF_3 plasma. Since HF^+ is not a significant fragment ion due to direct electron-impact dissociative ionization of CHF_3 , this ion is most likely produced by gas-phase ion–molecule or neutral–neutral reactions resulting in the formation of HF^+ or HF (with subsequent ionization). The detection of this ion is evidence of free fluorine scavenging by H atoms that are produced in plasmas generated in hydrogen-containing feed gases. HF^+ is not observed in CF_4 , C_2F_6 , and $c\text{-C}_4\text{F}_8$ plasmas.^{12,15}

In general, ions resulting from the direct ionization of CHF_3 account for less than one third of the total ion flux at the lower electrode. This confirms a significant degree of dissociation of the parent gas and significant secondary processes, such as ion–molecule and ion–surface reactions, occurring in the plasma. As will be discussed later, the large abundance of Si^+ , CO^+ , and HF^+ ions observed here is contrary to the results of earlier measurements made from the side of CHF_3 discharges in another GEC-ICP reactor.⁴

Interestingly, the relative abundance of Si-containing ions, presumably originating from the etching of the quartz surfaces in the system, was not observed to increase with the addition of the quartz annulus to the system. This would imply that these ions are produced on the upper quartz window surface, and that the presence of the additional Si in the quartz annulus does not affect this process.

Of the ions produced by direct ionization of CHF_3 , CF_3^+ , CHF_2^+ , CF_2^+ , and CF^+ all exhibit similar intensities, with CF_2^+ exhibiting the smallest intensity. While there is significant disagreement concerning the electron-impact partial ionization cross sections for CHF_3 ,²⁰ there is general agreement that the cross section for CF_2^+ production is substantially smaller than the cross sections for the formation of CF_3^+ , CHF_2^+ , and CF^+ . This is consistent with the observed relative intensities of these ions as sampled from the discharge.

Plasmas generated in CHF_3 produce many ions of comparable intensity, in contrast to CF_4 plasmas in which the ion flux consists primarily of CF_3^+ .¹⁵ Thus, as can be seen from Fig. 2, the ion flux produced in CHF_3 generally consists of ions of lower mass with a smaller F/C ratio compared to the ion flux in a CF_4 plasma. It has been suggested⁵ that gases which produce ions with higher F/C ratios etch SiO_2 at a higher rate in high density plasmas. Thus the detection of significant intensities of CF^+ , CF_2^+ , and CHF_2^+ (ions with low F/C ratios) from CHF_3 plasmas is consistent with the general observation of lower etching rates measured for CHF_3 plasmas when compared with CF_4 and C_2F_6 .^{5,18,19}

Figure 3(a) shows the absolute ion flux densities as a function of pressure for seven of the ions produced in a series of 200 W, CHF_3 plasmas generated with the quartz annulus in place. Also shown is the total ion flux density, which includes a contribution from the other less abundant ions. In general, the seven specific ions shown in Fig. 3 account for approximately 75% of the total ion flux density.

The only CHF_3 plasma data taken without the quartz annulus in place are shown in Fig. 3(b) for a gas pressure of

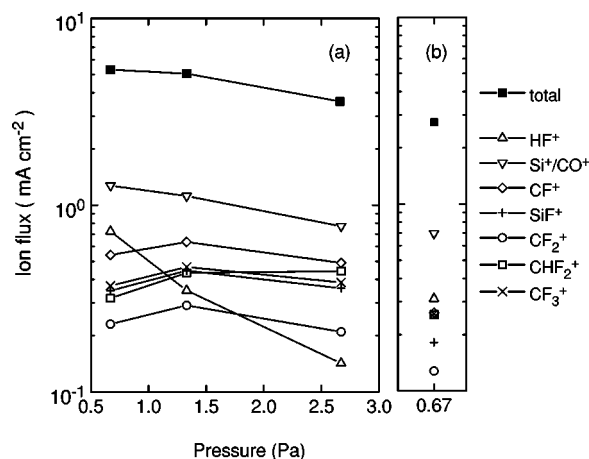


FIG. 3. Absolute mass-analyzed ion flux density striking the lower electrode of a GEC-ICP cell for CHF_3 plasmas as a function of gas pressure. The discharge power was maintained at 200 W. (a) Ion fluxes obtained with the quartz annulus in place around the upper quartz window. (b) Ion fluxes obtained without the quartz annulus. Stable plasmas could be maintained only for a narrow range of pressures near 0.67 Pa without the quartz annulus.

0.67 Pa (5 mTorr). Without the annulus in place, a stable discharge could be maintained in pure CHF_3 at 200 W only for a narrow range of pressures around 0.67 Pa. With the annulus in place, data were obtained for pressures ranging from 0.67 to 2.67 Pa (5–20 mTorr), thus demonstrating the extended operating range that is possible with the quartz ring in place. Stable plasmas at pressures exceeding 2.67 Pa could be generated in the cell with the ring in place, but they were not part of this investigation.

As can be seen by comparing the data taken at 0.67 Pa in Fig. 3, the total ion flux density increases by approximately a factor of 2 with the addition of the quartz annulus to the upper window. However, with some minor exceptions, the relative ion fluxes are nearly unchanged. As the pressure increases, the total ion current is observed to decrease. This decrease is primarily due to a reduction in the relative contributions of the “secondary” ions, Si^+ , CO^+ , and particularly HF^+ , to the total ion current. This is consistent with the potential role of ion–molecule reactions discussed below. In general, the ion flux densities for the CF_xH_y^+ ions remain nearly constant, or increase slightly, with increasing pressure.

A comparison can be made between the data presented here for a pure 200 W, CHF_3 plasma at 1.33 Pa (10 mTorr) and the data of Jayaraman *et al.*⁴ for similar plasma conditions. Jayaraman *et al.*⁴ measured relative ion intensities from CHF_3 plasmas generated in a GEC-ICP cell with silicon or resist-covered silicon wafers on the lower electrode. Interestingly, Jayaraman *et al.*⁴ observed CF_3^+ and CF^+ to be the dominant and next dominant detected ions, respectively. They also observed almost no Si-containing or CO^+ ions. These are significant discrepancies when compared with the data presented here for which the Si^+/CO^+ signal dominates at all pressures. The difference is especially noteworthy when one considers that the two reactors are nearly identical, and that the plasma conditions are ostensibly the same. One might even expect that Jayaraman *et al.*⁴ would have ob-

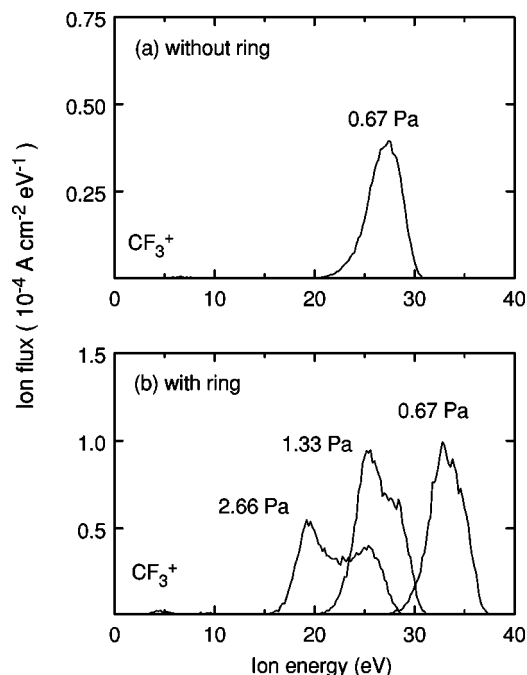


FIG. 4. Ion energy distributions for CF_3^+ ions sampled from CHF_3 plasmas at various pressures. (a) IED obtained for a plasma without the quartz annulus. (b) IEDs obtained with the quartz annulus in place.

served greater fluxes of Si-containing ions due to the the Si wafers present in their experiments. However, CHF_3 is known to exhibit a high SiO_2/Si etch ratio¹⁹ which is the result of a small Si etch rate. Therefore, the presence of a Si wafer would not necessarily increase the production of Si^+ ions in the discharge. A more likely explanation for the discrepancy is that the different position of the ion sampling orifices affects the observed ion flux composition.

For the present work, the sampling orifice is located in the center of the lower electrode which positions it near to the center of the plasma glow. For the work of Jayaraman *et al.*,⁴ the sampling orifice was on the side of the discharge nearly even with the outer edge of the electrodes. With the quartz annulus in place, the plasma glow is highly confined to the center of the electrodes. Thus, the side sampling orifice is located some distance from the “edge” of the glow which is near the inner radius of the quartz ring. While the cross sections for charge-exchange collisions of ions, such as Si^+ and CO^+ with CHF_3 , are unknown, cross sections for reactions between similar ions and neutrals, such as Ar^+ and CF_4 , are known to be substantial.²¹ The cross sections for the ions in this discharge are likely to be of comparable magnitude. This suggests that ions diffusing from the plasma glow to the sampling orifice on the side may undergo significant conversion to other ion species due to the high probability of experiencing a collision with a feed gas molecule. This would result in a significant reduction in the detection of ion flux due to non- CF_xH_y^+ ions, and would be consistent with the reduced intensity of these ions with increasing pressure observed in Fig. 3.

Figure 4(a) shows the measured ion energy distribution for CF_3^+ ions sampled from a 200 W, 0.67 Pa plasma in CHF_3 generated without the quartz annulus in place. The

IEDs for the other ions sampled from the same discharge are similar in shape, and all exhibit a mean energy of approximately 27 eV. Figure 4(b) shows the IEDs for CF_3^+ ions sampled from plasmas generated over a range of pressures with the quartz annulus in place. A comparison of the IEDs taken with and without the quartz ring for 0.67 Pa plasmas shows that the presence of the ring increases the mean ion energy by approximately 6 eV. This is consistent with an increase in the plasma density and a corresponding increase in the plasma potential. Additionally, the IEDs obtained with the quartz ring exhibit increased broadening due to increased rf modulation of the sheath voltage, which is attributable to a decrease of the ground sheath capacitance due to the smaller volume of the confined plasma glow interacting with the lower electrode. This broadening is most apparent at higher pressures and for the lighter ions.

For the present CHF_3 experiments, we have observed a greater tendency for film deposition to occur in the reactor when the quartz ring was removed from the system. This may be attributed to the lower ion energies observed in the plasma when no ring is present. Other experiments have indicated that CHF_3 plasmas convert from a deposition mode to an etching mode when ion energies increase to a moderate levels (approximately 30–50 eV).²² The ion energies observed here fall within this range for the low pressure plasmas generated with the quartz ring in place, thus suggesting a smaller amount of deposition under those conditions.

The mean ion energies observed here for CHF_3 at 0.67 Pa are similar to those observed previously for ions generated in CF_4 plasmas.¹⁵ In contrast, the mean energies of the ions generated in CHF_3 are significantly higher than those reported^{12,13} from C_2F_6 , $c\text{-C}_4\text{F}_8$, and CF_3I plasmas, presumably due to the greater electronegativity of the latter gases.

B. Plasmas in mixtures of CHF_3 and Ar

Rare gases, such as argon, may be added to more reactive plasma processing gases in order to increase sputtering yields and to vary the plasma characteristics without significantly influencing the reactive species present in the discharge. Figure 5 shows a mass spectrum of the ions sampled from a 200 W, 0.67 Pa plasma generated in a 50:50 mixture (by volume) of CHF_3 and Ar with the annulus in place. As for the CHF_3 plasmas, the mass spectrum is nearly identical to spectra (not shown) obtained without the quartz annulus. Additionally, with the exception of the now dominant Ar^+ peak, the mass spectrum in Fig. 5 is very similar to the spectrum shown in Fig. 2 for the 100% CHF_3 plasma.

Figure 6 shows the absolute total ion flux densities for a 50:50 mixture of CHF_3 and Ar as a function of pressure. Also shown are the mass-analyzed ion flux densities of the seven most abundant ions detected in the ion current. Figure 6(a) shows data obtained without the quartz annulus, and Fig. 6(b) shows data obtained with the annulus in place. For this gas mixture, the range of stable operation is about the same for both experimental arrangements, so additional performance comparisons can be made. As for the case of pure CHF_3 , the total absolute ion flux is observed to increase with

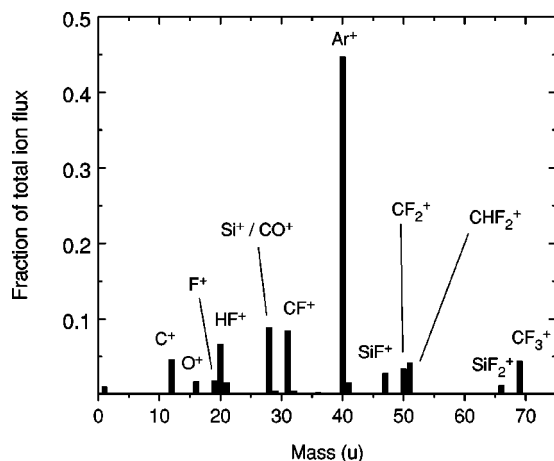


FIG. 5. Mass spectrum of ions sampled from a plasma generated in a 50:50 mixture of CHF_3 and argon. The plasma parameters were 200 W and 0.67 Pa (5 mTorr), and the quartz annulus around the upper quartz window (see Fig. 1) was in place. The mass spectra obtained under the same plasma conditions without the quartz annulus were nearly identical.

the use of the quartz annulus, but the composition of the ion flux remains relatively unaffected. Additionally, the general trends in the ion fluxes as the pressure increases are the same for both systems.

For both experimental arrangements, the Ar^+ ion is observed to be the dominant ion at all pressures. This is in contrast to the results of similar experiments^{12,15} with CF_4 and C_2F_6 for which the Ar^+ flux dominated only at 0.67 Pa, and $c\text{-C}_4\text{F}_8$ for which CF^+ was the dominant ion at all pressures.

Figure 7 shows the absolute total and mass-resolved ion flux densities for 200 W, 0.67 Pa plasmas as a function of the $\text{Ar}:\text{CHF}_3$ gas mixture composition. Again, a comparison of the data with and without the quartz ring shows an increase in ion flux with the ring, but with similar trends in flux with increasing CHF_3 concentration.

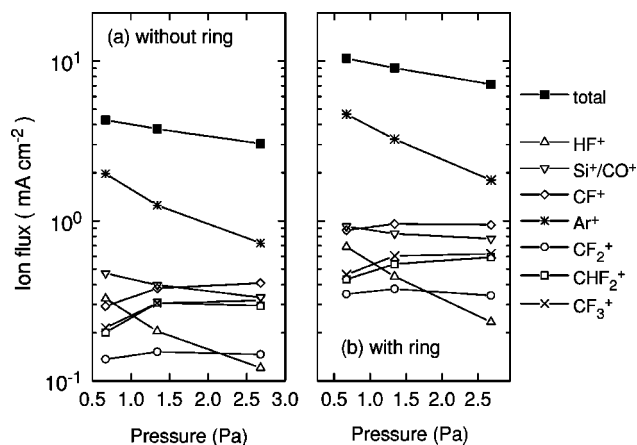


FIG. 6. Absolute total and mass-analyzed ion flux densities (for the seven most abundant ions) striking the lower electrode of a GEC-ICP cell for plasmas generated in a 50:50 mixture of CHF_3 and Ar as a function of gas pressure. The discharge power was maintained at 200 W. (a) Ion fluxes obtained without the quartz annulus. (b) Ion fluxes obtained with the quartz annulus in place around the upper quartz window.

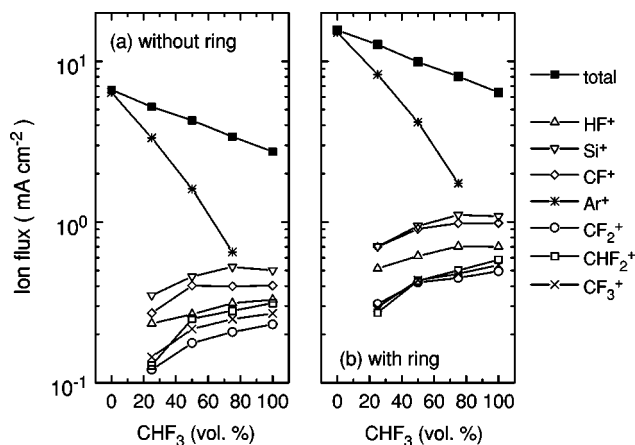


FIG. 7. Absolute total and mass-analyzed ion flux densities (for the seven most abundant ions) striking the lower electrode of a GEC-ICP cell for plasmas generated in mixtures of CHF_3 and Ar as a function of CHF_3 concentration (by volume). The discharge power was maintained at 200 W, and the gas pressure was held constant at 0.67 Pa. (a) Ion fluxes obtained without the quartz annulus. (b) Ion fluxes obtained with the quartz annulus in place around the upper quartz window.

The Ar^+ ion is again observed to be the dominant ion for all $\text{Ar}:\text{CHF}_3$ mixtures studied here. As with other fluorocarbon gases,^{12,15} the total ion current is seen to decrease with decreasing concentration of argon. However, in this case the reactive ion flux (non- Ar^+ ions) is observed to increase somewhat with increasing CHF_3 concentration, although not in proportion to the mixture. Recent measurements by Kim *et al.*²³ in a GEC-ICP cell exhibited nearly equal intensities of Ar^+ and CF_3^+ for 100 W plasmas in a mixture of 10% CHF_3 in Ar at pressures from 4.0 to 6.7 Pa. This is in potential conflict with our results shown in Fig. 7; however, the differences in power, pressure, and concentration between the present measurements and those of Kim *et al.*²³ make direct comparison difficult.

IV. CONCLUSIONS

The mass-analyzed ion flux densities have been measured for inductively coupled rf plasmas in pure CHF_3 and in mixtures of CHF_3 with Ar. For the case of pure CHF_3 , the dominant ion signal is due to a mixture of Si^+ and CO^+ ions. CHF_2^+ and CF^+ are the dominant CF_xH_y^+ ions, although CF_xH_y^+ ions generally account for less than one third of the total ion flux. The fact that such a small fraction of the detected ions can be attributed to direct ionization of the feed gas is important from the perspective of modeling CHF_3 plasmas. Obviously, surface reactions and gas-phase ion-molecule reactions play significant roles in the generation and transport of ions in this etching plasma.

The identity of the observed CF_xH_y^+ ions from the CHF_3 plasmas is consistent with observations of lower etch rates in CHF_3 plasmas than in plasmas using CF_4 or C_2F_6 gases^{5,19,24} because of a lower F/C ratio of the ions produced in CHF_3 . These ions are also consistent with the lower F/C composition detected in fluorocarbon films deposited by CHF_3 .

plasmas.^{18,22} The fluorocarbon film growth in CHF₃ has been shown to depend strongly on the material supplied by the ion flux.¹⁸

Investigations of the ion flux as a function of pressure indicate that the flux of reactive ion species to the surface is essentially constant with increasing pressure, thus indicating that the most efficient processes (in terms of the amount of reactive feed gas used) may be at lower pressures. Similarly, for mixtures of CHF₃ and Ar, the relative flux of reactive ions to the surface increased by less than a factor of 2, when the CHF₃ concentration was increased by a factor of 4. This again indicates that the increased use of the reactant feed gas does not necessarily result in a corresponding increase in the density of reactive ion species in the plasma. This has also been observed for CF₄, C₂F₆, and *c*-C₄F₈ plasmas.^{12,15}

Differences in the observed relative ion intensities between this experiment and those of Jayaraman *et al.*⁴ are potentially attributed to the different locations of the sampling orifice. Additional investigations of the influence of sampling ions from the side of the plasma versus sampling through the lower electrode must be performed to resolve this discrepancy. Determining which method most accurately probes the ion composition within the plasma glow is essential for comparison with predictive modeling results.

For some gases, such as CHF₃, the addition of a quartz annulus around the upper window of the GEC-ICP cell allows the generation of stable plasmas over a much broader range of pressures and powers than is possible in a standard GEC-ICP cell. Comparisons of the plasmas generated in the GEC-ICP cell with and without a quartz annulus indicate that the largest effect on the measured plasma parameters is an increase of the absolute ion flux by approximately a factor of 2. The relative intensities of the different ion species sampled at the grounded electrode do not change appreciably when the quartz annulus is used. In fact, for the plasma conditions studied here, the trends in the ion fluxes with changing pressures and gas mixtures are nearly identical for both experimental arrangements. There are some minor changes in the measured energies of the ions, but these are readily explainable in light of the smaller, more intense plasma that

is generated with the ring in place. This implies that the use of the quartz annulus is a reasonable modification to the GEC-ICP reactor geometry that expands the useful range of operation without substantially changing its performance.

- ¹N. R. Rueger, M. F. Doemling, M. Schaepekens, J. J. Beulens, T. E. F. M. Standaert, and G. S. Oehrlein, *J. Vac. Sci. Technol. A* **17**, 2492 (1999).
- ²B. Kim, K. H. Kwon, and S. H. Park, *J. Vac. Sci. Technol. A* **17**, 2593 (1999).
- ³L. G. Christophorou, J. K. Olthoff, and M. V. V. S. Rao, *J. Phys. Chem. Ref. Data* **26**, 1 (1997).
- ⁴R. Jayaraman, R. T. McGrath, and G. A. Hebner, *J. Vac. Sci. Technol. A* **17**, 1545 (1999).
- ⁵X. Li, M. Schaepekens, G. S. Oehrlein, R. E. Ellefson, L. C. Frees, N. Mueller, and N. Korner, *J. Vac. Sci. Technol. A* **17**, 2438 (1999).
- ⁶J. K. Olthoff and K. E. Greenberg, *J. Res. Natl. Inst. Stand. Technol.* **100**, 327 (1995).
- ⁷P. A. Miller, G. A. Hebner, K. E. Greenberg, P. S. Pochan, and B. P. Aragon, *J. Res. Natl. Inst. Stand. Technol.* **100**, 427 (1995).
- ⁸J. D. Bukowski, D. B. Graves, and P. Vitello, *J. Appl. Phys.* **80**, 2614 (1996).
- ⁹S. Rauf and M. J. Kushner, *J. Appl. Phys.* **82**, 2805 (1997).
- ¹⁰S. J. Choi and R. Veerasingam, *J. Vac. Sci. Technol. A* **16**, 1873 (1998).
- ¹¹E. Meeks, P. Ho, A. Ting, and R. J. Buss, *J. Vac. Sci. Technol. A* **16**, 2227 (1998).
- ¹²A. N. Goyette, Y. Wang, M. Misakian, and J. K. Olthoff, *J. Vac. Sci. Technol. A* (in press).
- ¹³A. N. Goyette, Y. Wang, and J. K. Olthoff, *J. Phys. D* **33**, 2004 (2000).
- ¹⁴P. J. Hargis *et al.*, *Rev. Sci. Instrum.* **65**, 140 (1994).
- ¹⁵J. K. Olthoff and Y. Wang, *J. Vac. Sci. Technol. A* **17**, 1552 (1999).
- ¹⁶Y. Wang and J. K. Olthoff, *J. Appl. Phys.* **85**, 6358 (1999).
- ¹⁷M. V. V. S. Rao, R. J. Van Brunt, and J. K. Olthoff, *Phys. Rev. E* **54**, 5641 (1996).
- ¹⁸G. S. Oehrlein, Y. Zhang, D. Vender, and M. Haverlag, *J. Vac. Sci. Technol. A* **12**, 323 (1994).
- ¹⁹G. S. Oehrlein, Y. Zhang, D. Vender, and O. Joubert, *J. Vac. Sci. Technol. A* **12**, 333 (1994).
- ²⁰L. G. Christophorou and J. K. Olthoff, *J. Phys. Chem. Ref. Data* **28**, 967 (1999).
- ²¹E. R. Fisher, M. E. Weber, and P. B. Armentrout, *J. Chem. Phys.* **92**, 2296 (1990).
- ²²G. M. W. Kroesen, H.-J. Lee, H. Moriguchi, H. Motomura, T. Shirafuji, and K. Tachibana, *J. Vac. Sci. Technol. A* **16**, 225 (1998).
- ²³J. S. Kim, M. V. V. S. Rao, M. A. Cappelli, M. Meyyappan, and S. P. Sharma, in *Proceedings of the International Symposium on Electron-Molecule Collisions and Swarms*, edited by Y. Hatano, H. Tanaka, and N. Kouchi, Tokyo, Japan, 18–20 July 1999, p. 127.
- ²⁴M. Schaepekens, T. E. F. M. Standaert, N. R. Rueger, P. G. M. Sebel, G. S. Oehrlein, and J. M. Cook, *J. Vac. Sci. Technol. A* **17**, 26 (1999).